Concentrated ion beam emitted from an enlarged cylindrical-anode-layer Hall plasma accelerator and mechanism

S. F. Geng,[1,2] D. L. Tang,[1] C. X. Wang,[1,2] X. M. Qiu,[1] and Paul K. Chu[2,a]

[1]*Southwestern Institute of Physics, Chengdu 610041, China*
[2]*Department of Physics and Materials Science, City University of Hong Kong, Tat Chee Avenue, Kowloon, Hong Kong, China*

An enlarged cylindrical-anode-layer Hall plasma accelerator with an outlet diameter of 150 mm is experimentally demonstrated to produce a concentrated ion beam, especially at a high discharge voltage, with a high current utilization efficiency of up to ∼0.9. Numerical investigation based on the three-dimensional particle-in-cell method is performed to study the ion dynamics and elucidate the origin of the ion beam characteristics. The simulation results reveal that the equipotential lines play an important role in the surface near the anode emitting the ions. The ion emitting surface is determined by the magnetic field lines near the anode and the magnetic mirror contributes to the concentrated beam significantly. The high current utilization efficiency results from the appropriate obliquity of the magnetic mirror. © 2013 American Institute of Physics. [http://dx.doi.org/10.1063/1.4788697]

I. INTRODUCTION

The Hall plasma accelerator, also known as Hall thruster, which is based on the discharge in the crossed E × B field, has been studied for several decades.[1–3] It is mainly used as an electrical propulsion unit in satellite stations for orbit transfer applications due to the attractive combination of high impulse, long lifetime, and high thrust efficiency. Commercially, it can be used as an ion source for surface cleaning, ion beam drilling, ion beam sputtering, and assisted deposition.[4] In a Hall plasma accelerator, the discharge occurs in the E × B field and electrons drift in the direction of E × B. It is called the Hall drift in which electrons impact neutral particles to ionize them. In this device, the electrons are magnetized, resulting in increased resistance and electron lifetime as well as promotion of ionization efficiency and plasma density. However, in a Hall plasma accelerator, ions are not created uniformly because of the different electrical potential and electric field at different locations. Ions generated from a Hall plasma accelerator have different kinetic energies and directions giving rise to both energy and beam divergence. In particular, beam divergence reduces the efficiency. In industrial units, some ions collide with the wall of a Hall plasma accelerator. This causes erosion of the device and emits impurities due to the large beam divergence.

Depending on the applications, the ion beam requirements are different. For instance, in ion-assisted applications,[5] a Hall ion source or Hall plasma accelerator that can deliver a broad beam is desired; whereas, in aerospace applications, an ion beam with little divergence is required. In some cases, a focused ion beam is required. For example, in the international thermonuclear experimental reactor (ITER) project, the high-ion-flux and high-heat-flux experiments require a focused ion beam generated by a specially designed anode-layer Hall plasma accelerator.[6] The ion beam profile

depends on the ion dynamics in a Hall plasma accelerator and is affected by the magnetic field significantly.[2,7,8] The magnetic field gradient influences the plasma flow in the channel due to effects on the potential distribution[9] and the magnetic field affects the conversion ratio of the ion beam current to discharge current in a cylindrical Hall plasma accelerator.[10] A positive-negative magnetic gradient can enhance the efficiency of the Hall plasma accelerator and experimental work[10,11] and numerical simulation[12,13] have been conducted. In this paper, we describe a novel enlarged cylindrical-anode-layer Hall plasma accelerator and the ion beam characteristics are evaluated systematically both experimentally and numerically.

II. HARDWARE CHARACTERISTICS AND EXPERIMENTAL DETAILS

The enlarged cylindrical-anode-layer Hall plasma accelerator with an outlet diameter of 150 mm is shown schematically in Fig. 1 in which the part surrounded by the dashed line will be simulated (to be discussed in Sec. III). A picture of the prototype is depicted in Fig. 2. The structure of the enlarged cylindrical-anode-layer Hall plasma accelerator is similar to that of the anode-layer Hall plasma accelerator.[10,11] In our design, in addition to the enlarged diameter, the anode is beveled so there is an oblique segment facing the discharge channel. The cylindrical magnetic poles, which play the role of the cathodes, introduce a magnetic mirror in the discharge channel. A magnetic mirror is used in many Hall plasma accelerators in which the electron motion is dictated by both the E × B drift and reflection from the magnetic mirror.[14] As shown in Fig. 3, the oblique face of the anode coincides with the slant of the magnetic mirror in our source and a good similarity between the equipotential contours and magnetic lines is obtained. The magnetic field flux density near the anode surface is 220 G.

The experiments were performed on the ion source having an inside dimension of 625 mm and length of 2300 mm

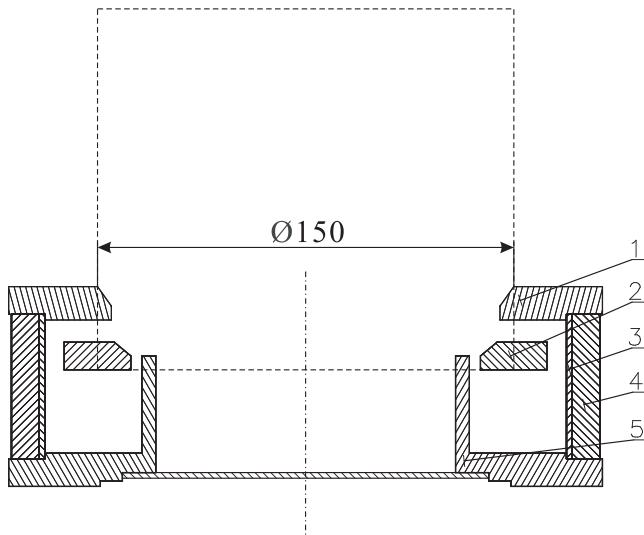a)Electronic mail: paul.chu@cityu.edu.hk.

FIG. 1. Schematic diagram of the enlarged cylindrical-anode-layer Hall plasma accelerator: (1) cathode/outer magnet pole, (2) anode, (3) inner shield, (4) permanent magnet, and (5) cathode/inner magnet pole.

FIG. 3. Magnetic field lines near the anode.

evacuated by two turbomolecular pumps. Before performing the experiments, the vacuum chamber was evacuated to a background pressure of 7.0×10^{-4} Pa. A series of probes were used to determine the ion beam profile and placed at 100 mm downstream from the outlet plane of the anode-layer Hall plasma accelerator. The distance between two neighboring probes was 40 mm and -50 V was applied to the probes. The ion beam profile was monitored at an argon pressure of 8.0×10^{-2} Pa (corresponding to an argon flow rate of 35 sccm) with the probes 100 mm away from the outlet plane as illustrated in Fig. 4. In the experiment, the discharge current rises from 0.03 A to 0.15 A when the voltage is increased from 600 V to 1300 V. At discharge voltages 600 V and 800 V, the ion beam had a full-width at half-maximum (FWHM) diameter of about 200 mm and 160 mm, respectively. The ion beam was divergent according to the outlet diameter 150 mm. When the discharge voltage
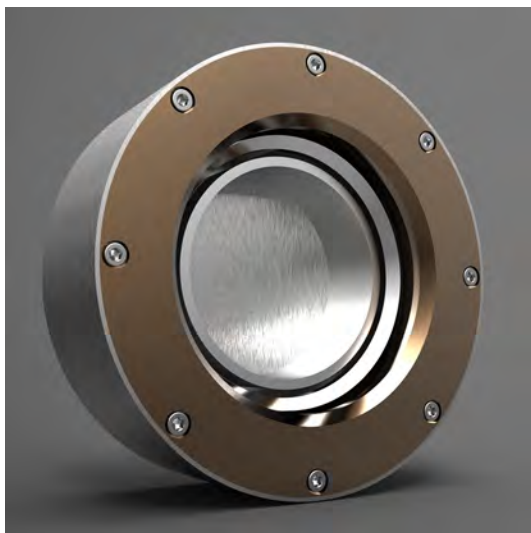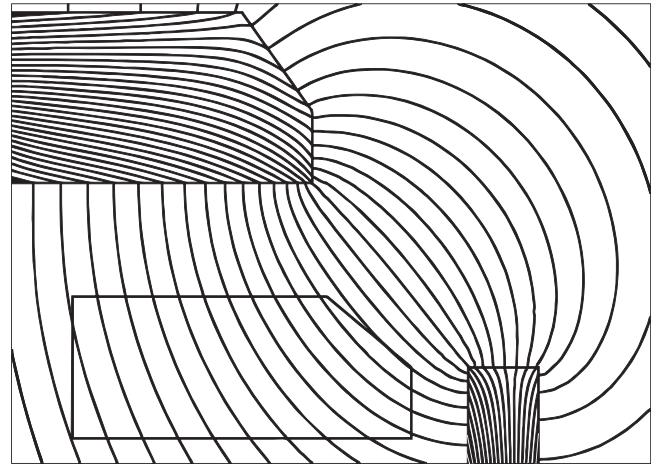
exceeded 1000 V, a concentrated ion beam was observed and the FWHM beam diameter was less than 100 mm, making it attractive to spacecraft applications as a component in the electrical propulsion system. When the voltage was raised from 800 V to 1000 V, the probe current increased quickly due to the rapid increase in the discharge current as the voltage was increased. The current utilization efficiency, the ratio of the ion beam current to discharge current, shown in Fig. 5 also contributed to the increase in the probe current. At most voltages, the current utilization efficiency was about 0.75–0.85 and the efficiency increased slowly with higher discharge voltage.

In addition to performing the experiments at an argon pressure of 8.0×10^{-2} Pa, the pressure was reduced to 3.0×10^{-2} Pa corresponding to an argon flow rate of 20 sccm with the discharge voltage set between 1000 V and 1900 V. The maximum discharge current was 66 mA at 1900 V. The photograph of the discharge in the cylindrical-anode-layer Hall plasma accelerator taken at the latter pressure is shown in Fig. 6, revealing that the discharge concentrates in the anode surface with blue light indicating higher ionization efficiency. The discharge takes place in an annular zone and the
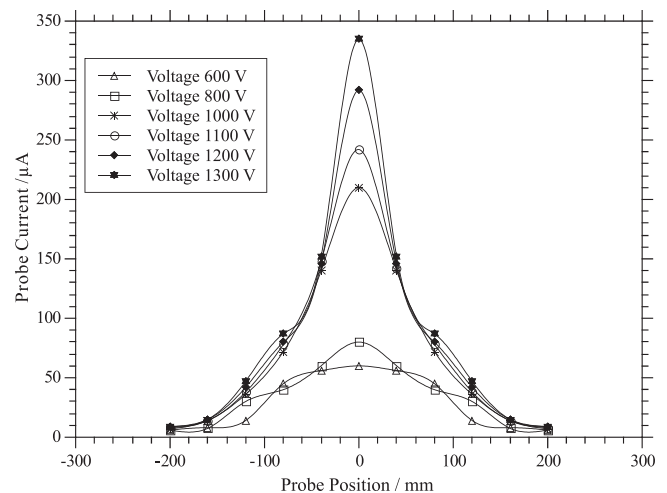

FIG. 2. Picture of the enlarged cylindrical-anode-layer Hall plasma accelerator prototype.

FIG. 4. Ion beam profile measured by a series of probes positioned at 100 mm from the outlet plane (Argon pressure $= 8.0 \times 10^{-2}$ Pa).
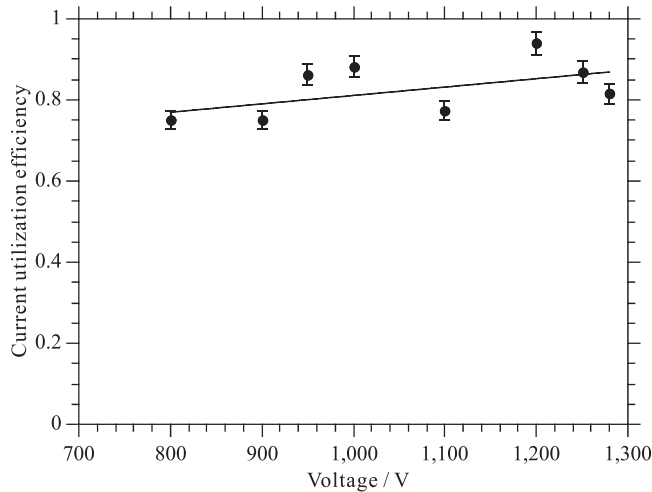
FIG. 5. Current utilization efficiency of the enlarged cylindrical-anode-layer Hall plasma accelerator at an argon pressure 8.0×10^{-2} Pa. The probe is placed at 250 mm downstream from the outlet of the Hall plasma accelerator.
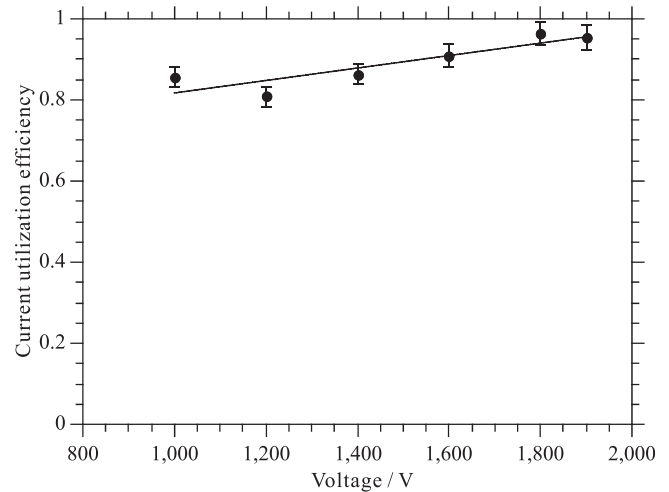

FIG. 7. Current utilization efficiency of the enlarged cylindrical-anode-layer Hall plasma accelerator at an argon pressure 3.0×10^{-2} Pa. The probe is placed at 250 mm downstream from the outlet of the Hall plasma accelerator.

beam emanates from the center of the anode-layer Hall plasma accelerator. The ion beam looks thin but highly concentrated, and at a higher voltage, the ion beam is more concentrated. A higher voltage not only condenses the ion beam but also increases the current efficiency, as shown in Fig. 7. At most voltages, the current utilization efficiency exceeds 0.8, and at a voltage higher than 1600 V, the current utilization efficiency is above 0.9. The general trend is that it rises with increasing voltage.

III. NUMERICAL SIMULATION

Numerical investigation is performed to elucidate the mechanism of the condensed ion beam described in Sec. II. The 3D particle-in-cell software VORPAL is adopted and the basic structure of the Hall plasma accelerator is depicted in Fig. 1 in which the part demarcated by the dashed lines is the region in which simulation is performed. The model is based

FIG. 6. Photograph of the discharge in the enlarged cylindrical-anode-layer Hall plasma accelerator.

on the 3D Cartesian coordinates and the simulated volume is 150 mm × 130 mm × 150 mm. The argon pressure is 3.0 × 10^{-2} Pa to simulate the discharge at a high voltage. The discharge voltages are between 1200 V and 2000 V. A higher argon pressure is not simulated because our computational facility is not able to handle both the high plasma density and large volume of the Hall plasma accelerator. Collisions included in the simulation are electron-neutral (ionization, excitation, and elastic scattering) as well as ion-neutral (charge exchange and elastic scattering). All the collisions are handled by Monte Carlo Collision (MCC) and the collisional cross sections are VORPAL built-in data.

In the simulation, the magnetic field data are imported to the particle-in-cell model. The data are assigned to grids and fixed in the simulation process. Some macro-particles are added to the model to simulate the real situations. When the simulation starts, these macro-particles initiate the discharge *via* impact ionization. In the model, there are 365 625 cells with size of 2 mm × 2 mm × 2 mm and 37 500 electron macro-particles in the ionization region as seed electrons to initiate the discharge. No macro-particles for ions exist in the beginning of the simulation. Because of the self-sustained property of the model, ion macro-particles can be generated by impact ionization. The simulation is performed using a time step of 1.0×10^{-10} s. The total discharge time simulated is 16 μs including 6 μs to establish the stable discharge.

IV. RESULTS AND DISCUSSION

Figs. 8(a) and 8(b) show the simulated electron and ion distributions, respectively, which are quite different from those of traditional small-diameter cylindrical-anode-layer Hall plasma accelerators.[12,13] The electrons do not occupy the central zone but rather adhere closely to the anode. The electron distribution is consistent with the experimental data shown in Fig. 6 and the ion distribution in Fig. 8(b) shows an obvious ion beam along the central axis. To investigate the beam characteristics by simulation, the ion flux diagnostics is applied to the boundary perpendicular to the central axis.
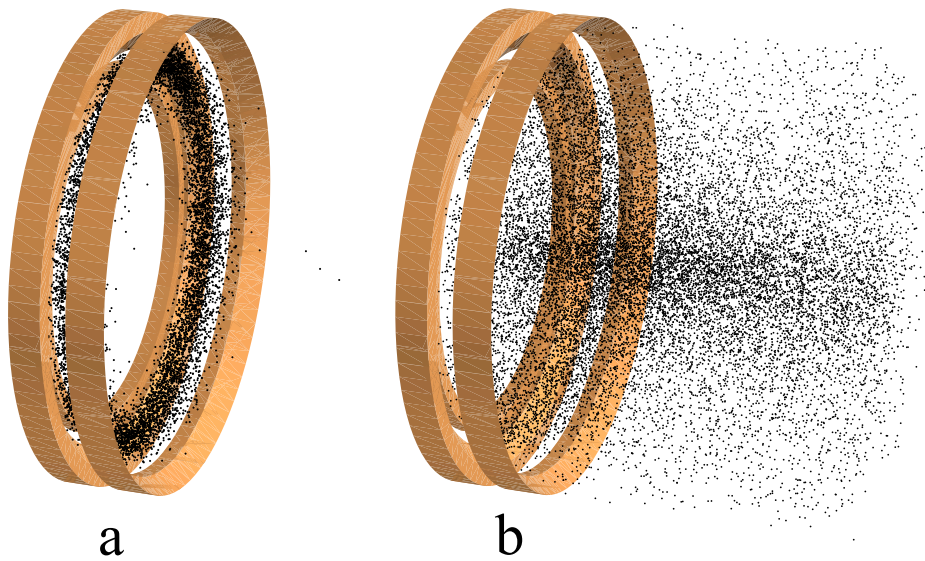
FIG. 8. (a) Simulated electron distribution and (b) ion distribution.

Ions go through this boundary and leave the simulation region. The ion flux density distribution along the diameter is illustrated in Fig. 9. Both the experimental and simulation results show that the high flux density is at the center.

The experimental study and numerical investigation reveal that the cylindrical-anode-layer Hall plasma accelerator produces a concentrated and thin ion beam. In this device, the electrons are magnetized but ions are not confined and so the ion trajectory depends on two factors: the position at which the ion is formed originally and the potential distribution in the Hall plasma accelerator. Fig. 8(a) shows that most of the ions are created near the anode surface and the potential distribution at a discharge voltage of 1600 V is exhibited in Fig. 10. The contours start from 30 V and the step of two neighboring equipotential lines is 15 V.

In the anode layer where most ions are formed, there is very large potential drop of about 150 V/mm and the contours near the anode are similar to the magnetic field lines here. The equipotential lines near the anode layer are generally regarded to dictate the emitting surface and they also determine the direction at which an ion is accelerated. Further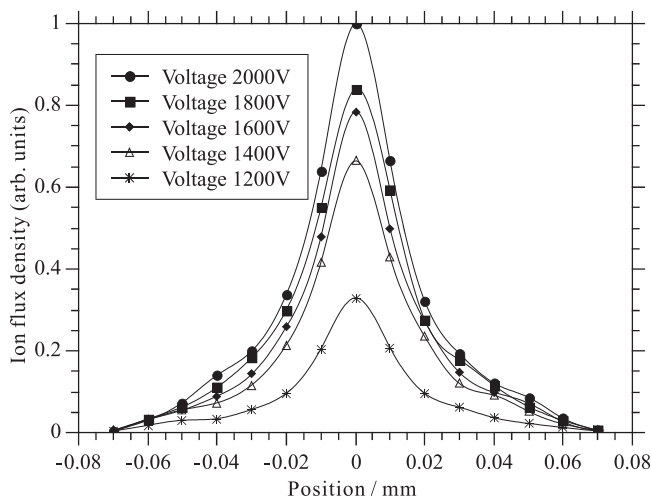more, as shown in Fig. 10, there is a potential barrier at the center of the Hall plasma accelerator. The potential barrier has a long and narrow shape and a peak of ∼195 V.

The final ion distribution and ion beam characteristics result from the potential distribution and the ion trajectories are shown in Fig. 11 in which the 3D illustration is shown at the lower right corner. For simplicity, Fig. 11 only shows the results from a slice with a thickness of 6 mm. The emitting surfaces cause the beam to crossover in the center of the Hall plasma accelerator. The crossover is an important factor giving rise to the high ion flux density distribution along the axis. In addition, some ions do not cross the axis, but approach the axis asymptotically due to the effect of the potential barrier. This behavior also leads to the concentrated ion beam in Hall plasma accelerator.

In the device, electrons drift in an annular and narrow orbit closed to the anode surface. In this narrow area,

$$\vec{v} = \frac{\vec{E} \times \vec{B}}{B^2}. \tag{1}$$

FIG. 9. Simulated ion flux density at the boundary along the diameter of the Hall plasma accelerator (100 mm downstream from the outlet).
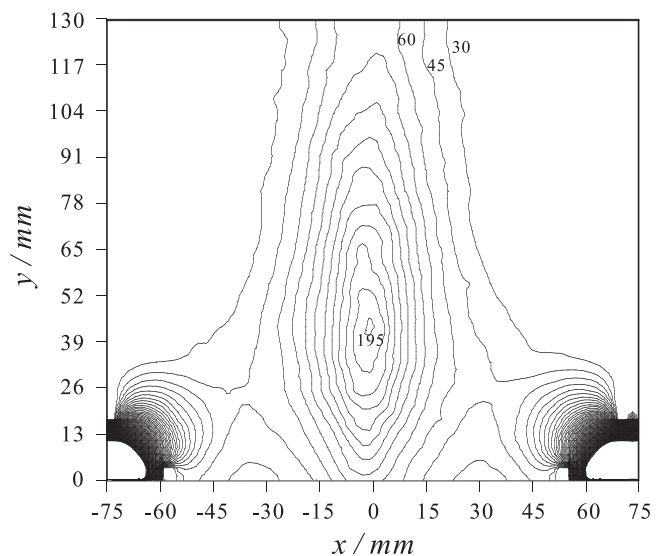

FIG. 10. Potential distribution at on the central plane of the enlarged cylindrical-anode-layer Hall plasma accelerator at a discharge voltage 1600 V.
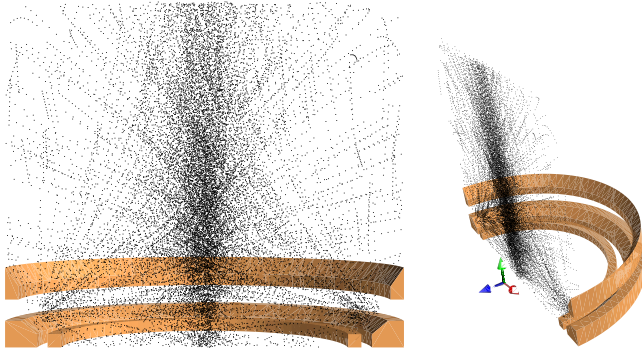
FIG. 11. Ion trajectories with the illustrated objects being the ions in a thin slice. The position of the slice is shown in the 3D diagram at the lower right corner.

This is the equation for Hall drift and from Eq. (1), we obtain

$$\vec{E} = -\vec{v} \times \vec{B}. \qquad (2)$$

Also we have

$$\vec{E} = -\nabla \varphi. \qquad (3)$$

In these equations, the symbols have their usual meaning. The simple relationship between the magnetic field and electrical potential is

$$\nabla \varphi = \vec{v} \times \vec{B}. \qquad (4)$$

Hence, in the area near the anode surface, the equipotential lines are almost equal to the magnetic field lines. We can estimate the potential distribution close to the anode surface using the magnetic field, as illustrated by the simulation results (potential distribution) in Fig. 10. There are similarities between the equipotential lines in Fig. 10 and magnetic field lines in Fig. 3 and hence, the magnetic field contributes to the concentrated ion beam significantly. The high current utilization efficiency can be easily explained by the ions trajectories. It can be observed from Fig. 11 that only a small fraction of ions goes downstream in the Hall plasma accelerator and there are almost no ions impacting the cathode.

V. CONCLUSION

A concentration ion beam is produced by a novel enlarged cylindrical-anode-layer Hall plasma accelerator with an outlet diameter of 150 mm. The current utilization efficiency is 0.75–0.85 at a pressure of 8.0×10^{-2} Pa and voltage of less than 1300 V. At a lower pressure of 3.0×10^{-2} Pa and discharge voltage up to 1900 V, a thin and highly concentrated ion beam is produced. The current utilization efficiency reaches 0.85–0.96 and increases with higher voltage. Numerical investigation based on the three-dimensional particle-in-cell method is performed to elucidate the ion dynamics observed in the experiments. The simulation results reveal that the ion beam characteristics result from the equipotential lines which play a key role in the ion emitting surface near the anode. The ion emitting surface is determined by the magnetic field lines near the anode and the magnetic mirror contributes to the concentrated beam significantly. In addition, the enlarged cylindrical-anode-layer Hall plasma accelerator boasts low wall erosion due to less ion impact as a result of ion beam condensation and high current utilization efficiency.

[1]H. R. Kaufman, AIAA J. **23**, 78 (1985).
[2]V. V. Zhurin, H. R. Kaufmann, and R. S. Robinson, Plasma Sources Sci. Technol. **8**, R1 (1999).
[3]A. Smirnov, Y. Raitses, and N. J. Fisch, Phys. Plasmas **14**, 057106 (2007).
[4]A. Anders, Surf. Coat. Technol. **200**, 1893 (2005).
[5]H. R. Kaufman and J. E. Harper, "Ion assist applications of broad-beam ion sources," in *Advances in Thin Film Coatings for Optical Applications*, edited by J. D. T. Kruschwitz and J. B. Oliver (SPIE, Bellingham, WA, 2004).
[6]O. Girka, I. Bizyukov, K. Sereda, A. Bizyukov, M. Gutkin, and V. Sleptsov, Rev. Sci. Instrum. **83**, 083501 (2012).
[7]A. I. Morozov, Sov. Phys. Dokl. **10**, 775 (1966).
[8]M. Keidar, A. D. Gallimore, Y. Raitses, and I. D. Boyd, Appl. Phys. Lett. **85**, 2481 (2004).
[9]M. Keidar and I. D. Boyd, Appl. Phys. Lett. **87**, 121501 (2005).
[10]D. L. Tang, J. Zhao, L. S. Wang, S. H. Pu, C. M. Cheng, and P. K. Chu, J. Appl. Phys. **102**, 123305 (2007).
[11]D. L. Tang, L. S. Wang, S. H. Pu, C. M. Cheng, and P. K. Chu, Nucl. Instrum. Methods Phys. Res. B **257**, 796 (2007).
[12]S. F. Geng, X. M. Qiu, C. M. Cheng, P. K. Chu, and D. L. Tang, Phys. Plasmas **19**, 043507 (2012).
[13]D. L. Tang, S. F. Geng, X. M. Qiu, and Paul K. Chu, Phys. Plasmas **19**, 073519 (2012).
[14]J. Perez-Luna, N. Dubuit, L. Garrigues, G. Hagelaar, and J. P. Boeuf, IEEE Trans. Plasma Sci. **36**, 1212 (2008).